



A Thermomechanical Model of an Elastic Particle in a Metallic Matrix

J. Lachowski ^{*,a}, J. M. Borowiecka-Jamrozek ^b

^a Faculty of Management and Computer Modelling, Department of Applied Computer Science and Applied Mathematics, Kielce University of Technology, Al. Tysiąclecia PP. 7, 25-314 Kielce, Poland

^b Faculty of Mechatronics and Mechanical Engineering, Department of Applied Computer Science and Armament Engineering, Kielce University of Technology, Al. Tysiąclecia PP. 7, 25-314 Kielce, Poland

* Corresponding author. E-mail address: jlach@tu.kielce.pl

Received 27.08.2017; accepted in revised form 28.11.2017

Abstract

This paper deals with numerical and analytical modelling of a diamond or silicon particle embedded in a metallic matrix. The numerical model of an elastic particle in a metallic matrix was created using the Abaqus software. Truncated octahedron-shaped and spherical-shaped diamond particles were considered. The numerical analysis involved determining the effect of temperature on the elastic and plastic parameters of the matrix material. The analytical model was developed for a spherical particle in a metallic matrix. The comparison of the numerical results with the analytical data indicates that the mechanical parameters responsible for the retention of diamond particles in a metal matrix are: the elastic energy of the particle, the elastic energy of the matrix and the radius of the plastic zone around the particle. An Al-based alloy containing 5% of Si and 2% of Cu was selected to study the mechanical behaviour of silicon precipitates embedded in the aluminium matrix. The model proposed to describe an elastic particle in a metallic matrix can be used to analyze other materials with inclusions or precipitates.

Keywords: Metallography, Mechanical properties, Synthetic diamond, Hot pressing, Silicon precipitate

1. Introduction

This paper discusses a mathematical model of an elastic particle in an elastic-plastic metallic matrix. The mechanical state of such a particle embedded in a metal matrix results from the cooling of the sintered or composite material required by the manufacturing process [1]. If the coefficient of thermal expansion of the particle material is lower than that of the matrix, the particle is compressed by the contracting matrix. The stress in the elastic particle is constant, while the stress around it decreases to zero rapidly. When the difference in the coefficient of thermal expansion is larger and there is a sufficient drop in temperature, the plastic zone around the particle is formed.

A particularly large difference in the coefficient of thermal expansion is observed between diamond particles or silicon

precipitates and metallic matrixes. For diamond and silicon, the coefficient of thermal expansion is very low. For metals, on the other hand, its value is several times higher. This is the reason why a diamond particle in a cobalt matrix [2] and a silicon precipitate in an Al5%Si alloy [3] were selected for the analysis.

2. Numerical model of a diamond particle in a metallic matrix

Depending on the synthesis conditions, diamond crystallization leads to the formation of crystals with shapes ranging from a cube to an octahedron [1]. Intermediate shapes of a diamond crystal are: a truncated cube, a cuboctahedron and a

truncated octahedron. The truncated octahedron is the most spherical object of all the Archimedean solids (semi-regular convex polyhedrons).

The models of a diamond crystal embedded in a metallic matrix and protruding from its surface (Figure 1) were discussed in [1]. The values of the numerically calculated pressure inside a diamond particle [1] coincided with those observed in the experiments [4].

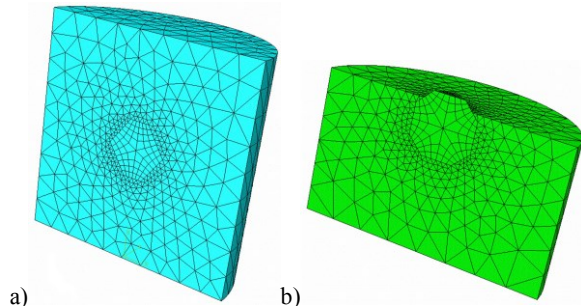


Fig. 1. Models of a diamond particle: a) fully embedded in the matrix, b) protruding from its surface

The simulation results show that it is possible to select parameters that are slightly dependent on the particle shape and size. They are the pressure inside the diamond particle and the plastic zone size around it [1].

In this study, the preliminary numerical analysis was conducted for a cobalt matrix. The mechanical parameters of the matrix were determined using the corresponding average values obtained for the sintered SMS (Submicron Size) and EF (Extra Fine) cobalt powders (Table 1, Figure 2) [2]. The elastic modulus E and the Poisson ratio ν of diamond were 1050 GPa and 0.1, respectively. The hot pressing process to produce the sintered materials was assumed to take place at a temperature of 850 °C and a pressure of 35 MPa. The average values of the coefficient of thermal expansion used for the cobalt matrix and the embedded diamond particles were $15.2 \cdot 10^{-6} \text{ K}^{-1}$ and $3 \cdot 10^{-6} \text{ K}^{-1}$, respectively.

The simulations were carried out by means of the Abaqus [5] program. The results obtained for a truncated octahedron-shaped particle were compared with those registered for a spherical particle (Figure 3). The particles were identical in volume, which corresponded to that of a sphere with a radius of 172.5 μm . The simulation results are shown in Table 2. In this table and in the next tables, the radius of the plastic zone is divided by the radius of the sphere R .

Table 1.

Mechanical properties of the modelled cobalt matrix

Modulus of elasticity E [GPa]	Poisson ratio ν	Yield strength σ_Y [MPa]	Tensile strength σ_T [MPa]	Elongation A [%]
205	0.3	519	1041	13.9

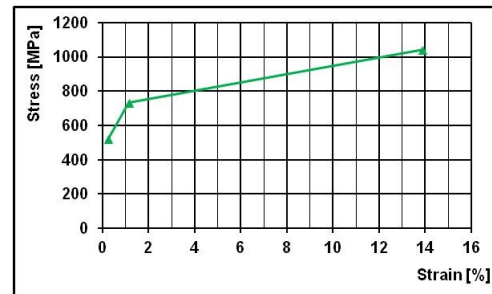


Fig. 2. Stress-strain curve for the cobalt matrix

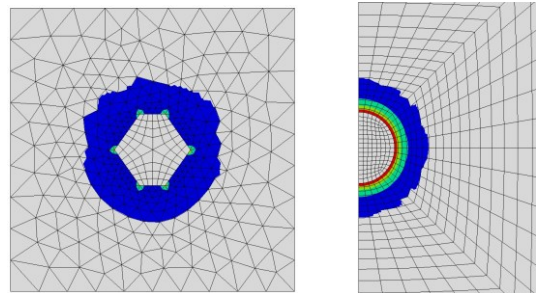


Fig. 3. Plastic zones around a truncated octahedron-shaped (left) and spherical (right) particles

As can be seen from Table 2, there are no significant differences in results between the truncated octahedron-shaped particle and the spherical one. The plastic zone surrounding the truncated octahedron particle is almost spherical and has a well defined radius (Fig. 3). Thus, the shape of the diamond particle in the cobalt matrix can be approximated as a sphere.

Table 2.

Simulation results for the truncated octahedron-shaped and spherical-shaped particles

Shape of particle	Pressure inside particle [MPa]	Coefficient of plastic zone r_p/R	Elastic energy of particle [mJ]
Truncated octahedron	1081	1.85	0.0298
Sphere	1121	1.80	0.0319

3. Mathematical model of a diamond particle in a metallic matrix

An analytical model of a spherical elastic particle in an elastic ideally plastic matrix was presented in [1]. The elastic stresses in the particle and the matrix were determined using the Lamé solution [6]; the plastic zone around the particle was defined from the results provided in [7]. The radius of the plastic zone was calculated using the following equation [1]:

$$(1-\nu_p)\frac{r_p^3}{R^3}-2\left((1-2\nu_m)-\frac{E_m}{E_p}\right)\left(\ln\left(\frac{r_p}{R}\right)+\frac{1}{3}\right)=\frac{E_m}{\sigma_0}(\alpha_m-\alpha_p)\Delta T \quad (1)$$

where:

E – elastic modulus, ν – Poisson ratio, index p – particle parameters, index m – matrix parameters, R – radius of the diamond particle, r_p – radius of the plastic zone around the particle (Figure 4), α_m and α_p – coefficients of thermal expansion of the matrix and the particle, respectively, ΔT – drop in temperature during cooling after hot pressing and σ_0 – yield stress of the matrix.

The radial and hoop stresses in the plastic zone can be written as follows:

$$\sigma_{rr} = -2\sigma_0 \ln\left(\frac{r_p}{r}\right) - \frac{2}{3}\sigma_0 \quad (2)$$

$$\sigma_{\varphi\varphi} = -2\sigma_0 \ln\left(\frac{r_p}{r}\right) + \frac{1}{3}\sigma_0 \quad (3)$$

Since the stress in a spherical particle is constant, the pressure inside can be calculated immediately from [1]

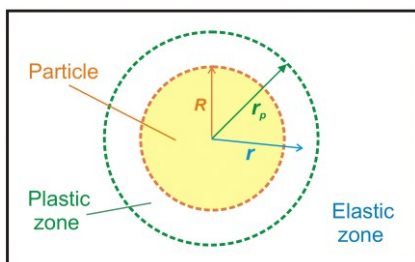


Fig. 4. Model of a matrix-embedded particle

$$p_p = 2\sigma_0 \ln\left(\frac{r_p}{R}\right) + \frac{2}{3}\sigma_0 \quad (4)$$

The stress in the elastic region outside the plastic zone ($r > r_p$ at Fig. 3) decreases as $1/r^3$

$$\sigma_{rr} = -\frac{2E_m}{1+\nu_m} \frac{b}{r^3} \quad \sigma_{\varphi\varphi} = \frac{E_m}{1+\nu_m} \frac{b}{r^3} \quad (5)$$

where the constant b is defined as follows

$$b = \frac{1}{3}\sigma_0 \frac{1+\nu_m}{E_m} r_p^3 \quad (6)$$

The mathematical model was verified by comparing the analytical results with the simulation results for the 2D numerical model of the spherical particle (Table 3).

Table 3.

Simulation results for the numerical and analytical model for the cobalt matrix

Type of model	Pressure inside particle [MPa]	Coefficient of plastic zone r_p/R	Elastic energy of particle [mJ]	Density of energy [mJ/mm ³]
Numerical	1121	1.80	0.0319	1.421
Analytical	1118	1.70	0.0307	1.368

The numerical analysis involved studying the effect of temperature on the elastic and plastic parameters of the cobalt matrix. The change in the modulus of elasticity with temperature was determined in the same way as for steels [8]. The modulus E was assumed to change linearly from 205 GPa at 20 °C to 135 GPa at 900 °C. The stress-strain curve (Fig. 2) was plotted assuming that, at 927 °C, the yield strength decreased 5.3 times and the tensile strength decreased 4.6 times [9]. The calculation results of the temperature-independent model and the temperature-dependent model were compared in Table 4.

Table 4.

Temperature-independent model vs. temperature-dependent model

Type of model	Pressure inside particle [MPa]	Coefficient of plastic zone r_p/R	Elastic energy of particle [mJ]	Maximum $PEEQ^*$ [%]
Temperature-independent	1121	1.80	0.0319	1.68
Temperature-dependent	1116	1.86	0.0316	1.66

* the Abaqus variable $PEEQ$ [9] is the equivalent plastic strain

$$\bar{\varepsilon} = \sqrt{\frac{2}{9}((\varepsilon_I - \varepsilon_{II})^2 + (\varepsilon_{II} - \varepsilon_{III})^2 + (\varepsilon_{III} - \varepsilon_I)^2)}$$

with ε_I , ε_{II} and ε_{III} being the principal strain components.

The parameters analyzed in Table 4 are meaningfully dependent on the mechanical properties at ambient temperature.

4. Model of a silicon particle in an aluminum matrix

The structure and tensile strength of AlSi5Cu2 alloy containing 5% of silicon and 2% of copper by weight were analysed in [3]. The material was produced in accordance with PN-EN 1706:2001. The alloy was annealed for 3 h at a temperature of 500 °C. The tensile tests were performed using an Instron universal testing machine. Both smooth and U-notched specimens were employed.

The structure of the material was examined by means of a JEOL JSM 5400 scanning electron microscope equipped with an ISIS 300 X-ray spectrometer (Figure 5). The chemical compositions of the silicon precipitates and the aluminium matrix are shown in Table 4. As can be seen from Fig. 5, the silicon

particles are not uniformly distributed throughout the structure; they form clusters.

Table 5.

Al, Si and Cu concentrations in Si precipitates and aluminium matrix

Element	Al	Si	Cu
Silicon precipitate	3.50	96.50	
Al matrix	95.34	1.01	2.28

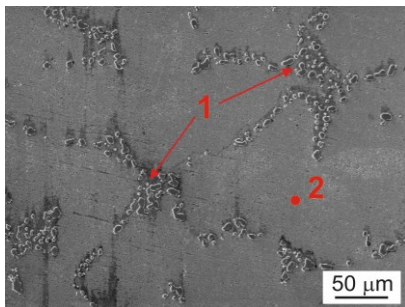


Fig. 5. Microstructure of the Al-5%Si alloy etched with 3% HF, 1 - Si precipitates, 2- Al matrix

The numerical and analytical calculations were performed for a 10 μm silicon particle embedded in an aluminum matrix. A drop in temperature from 500 °C to 20 °C was assumed. The numerical and analytical calculations were based on the material data from Table 6. The calculation results are provided in Table 7.

Table 6.

Properties of the aluminum and silicon phases

Phase	E [GPa]	ν	σ _Y / σ _T [MPa]	A [%]	α[K ⁻¹]
Silicon precipitate	107	0.4			4.35·10 ⁻⁵
Al matrix	70	0.33	273/320	2.24	2.41·10 ⁻⁵

Table 7.

Numerical and analytical results for the Al5%Si alloy

Type of model	Pressure inside particle [MPa]	Coefficient of plastic zone r _p /R	Elastic energy of particle [mJ]	Density of energy [mJ/mm ³]
Numerical	454	1.70	0.300·10 ⁻⁷	0.0573
Analytical	468	1.69	0.322·10 ⁻⁷	0.0615

The research presented in [3] was supplemented with a numerical failure analysis conducted with the Abaqus program ver. 6.14 [6]. A computer simulation of the stress state in notched specimens was carried out using the Gurson-Tvergaard-Needleman model (GNT model) for a porous solid [11,12]

$$\Phi = \frac{\sigma_{red}^2}{\sigma(\varepsilon)^2} + 2f^* \cosh\left(-\frac{3\sigma_m}{2\sigma(\varepsilon)}\right) - (1 + (f^*)^2) = 0 \quad (7)$$

where σ_{red} is the stress reduced according to the Huber-Mises hypothesis, σ_m is the mean stress and $\sigma(\varepsilon)$ is the stress resulting from the actual stress-strain curve. The function f^* represents a rapid decrease in the transmitted load with increasing void volume fraction

$$f^*(f) = f \quad \text{for } f \leq f_c \quad (8a)$$

$$f^*(f) = f_c + \frac{1-f_c}{f_F-f_c}(f-f_c) \quad \text{for } f > f_c \quad (8b)$$

where f is the void volume fraction, f_c is the critical value of the void volume fraction above which the process of void coalescence occurs and the material strength drops rapidly. The parameter f_F is the void volume fraction at fracture [13].

The model assumes that an increase in the void volume fraction f occurs as a result of the growth of voids present in the material and the formation of voids on the Si particles (cracking and decohesion of the particles) with increasing plastic strain [14]. In the numerical approach, the nucleation of new voids was determined using the following formula

$$df_n = A \cdot d\varepsilon^{pl} \quad (9)$$

where the coefficient A represents the nucleation of voids in the form of normal distribution around a certain value of the mean strain [15]

$$A = \frac{f_N}{s_N \sqrt{2\pi}} \exp\left[-\frac{1}{2} \left(\frac{\varepsilon - \varepsilon_N}{s_N}\right)^2\right] \quad (10)$$

where f_N represents the volume fraction of void-nucleating particles, ε_N is the mean plastic strain at which nucleation occurs and s_N is the standard deviation of nucleation.

The simulation conducted with Abaqus [5] using the GNT model (7) aimed at reconstructing the stress-strain curves for notched specimens. The theoretical stress-strain curves were compared with the experimental stress-strain curves taking into consideration the following parameters: the initial volume fraction f_0 , the volume fraction of void-nucleating particles f_N , the mean nucleation strain ε_N , the standard deviation of nucleation s_N , the critical void volume fraction f_c and the void volume fraction at fracture f_F . The best results were obtained for the values presented in Table 8.

The parameters provided in columns 3-6 of Table 8 were selected to best match the computer simulation results to the experimental curve [3]. For the analyzed system of silicon precipitates in the aluminum-silicon alloy, the parameters can be determined using the model of an elastic particle in a metallic matrix described in Section 3.

Previous simulations conducted for a system of Si precipitates in an AlSi alloy [14] did not take into account the initial state of the particle (Table 7).

Table 8.

Material parameters used in the computer simulation

f_0	f_N	ε_N	S_N	f_C	f_F
0.02	0.046	0.022	0.01	0.045	0.25

5. Conclusions

An elastic particle located inside a metal matrix can be characterized by the following parameters:

- the pressure inside the particle,
- the elastic energy of the particle or density of the energy,
- the radius of the plastic zone.

The pressure inside the particle and the density of the elastic energy are parameters independent of the particle size. They can be used to determine the mechanical properties of the elastic-particles metallic-matrix system. Similarly, the radius of the plastic zone reduced to the radius of the particle R can be employed. All these parameters can be applied as indices of the diamond particle retention in the metal matrix.

The model proposed to describe an elastic particle in a metallic matrix can be used to analyze other materials with inclusions or precipitates when their coefficient of thermal expansion is lower than that of the metallic matrix.

References

- [1] Lachowski, J. & Borowiecka-Jamrozek, J. (2017). Modelling Thermomechanical Response of a Diamond Particle in a Metallic Matrix. *Engineering Transactions*. 65(1), 105-112.
- [2] Borowiecka-Jamrozek, J. (2013). Engineering structure and properties of materials used as a matrix in diamond impregnated tools. *Archives of Metallurgy and Materials*. 58(1), 5-8. DOI: 10.2478/v10172-012-0142-0.
- [3] Borowiecka-Jamrozek, J. & Lachowski, J. (2014). Analysis of Stresses in Al-5%Si Alloy under Loading Conditions. *Journal of Achievements in Materials and Manufacturing Engineering*. 65(1), 26-31.
- [4] Akyuz, D.A. (1999). *Interface and microstructure in cobalt-based diamond tools containing chromium*. PhD thesis, Ecole Polytechnique Federale de Lausanne, Lausanne, 105-108.
- [5] SIMULIA Dassault System, Abaqus analysis user's guide, ver. 6.14 (2014). Computer Cluster at Kielce University of Technology.
- [6] Landau, L.D. & Lifszitz, E.M. (1975). *Theory of Elasticity*. 2nd ed., Pergamon Press Ltd., Oxford, 20-21.
- [7] Hill, R. (1950, reprinted 2009). *The Mathematical Theory of Plasticity*. Clarendon Press. Oxford. 97-101.
- [8] Hampel, C.A. ed., (1961). *Rare Metals Handbook*, Reinhold Publishing Corporation, London, 124-126.
- [9] Rosler, J., Harders, H., Baker, M. (2007). *Mechanical Behaviour of Engineering Materials*. Springer-Verlag, Berlin. 60-62.
- [10] SIMULIA Dassault System, Abaqus Analysis User's Guide, Output Variable and Element Indexes, ver. 6.14 (2014).
- [11] Gurson, A.L. (1977). Continuum theory of ductile rupture by void nucleation and growth. *Journal of Engineering Materials Technology*. 99, 2-15.
- [12] Kossakowski, P.G. (2012). The prediction of ductile fracture to S235JR steel using the stress modified critical strain and Gurson-Tvergaard-Needleman models. *Journal of Materials in Civil Engineering*. 24, 1492-1500.
- [13] Neimitz, A. & Grzegorzczak, A. (2014). Numerical analysis of the failure processes of plates made of S 960 QC steel. *Key Engineering Materials*. 598, 184-189.
- [14] Huber, G., Brechet, Y. & Pardoën, T. (2005). Predictive model for void nucleation and void growth controlled ductility in quasi-eutectic cast aluminium alloys. *Acta Materialia*. 53, 2739-2749.
- [15] Koplik, J. & Needleman, A. (1988). Void coalescence in porous plastic solids. *International Journal of Solids Structures*. 24(8), 835-85